EFFECTS OF TURBULENT FLOW CHARACTERISTICS ON WIND-INDUCED NOISE GENERATION IN SHIELDED MICROPHONES

Vahid Alamshah[1], Anthony Zander[2] and Valeri Lenchine[3]

[1]Resonate Acoustics
Adelaide SA 5000, Australia
Email: vahid.alamshah@resonateacoustics.com

[2]School of Mechanical Engineering
University of Adelaide, Adelaide SA 5000, Australia
Email : anthony.zander@adelaide.edu.au

[3]Science and Assessment Division
SA Environment Protection Authority, GPO Box 260, Adelaide SA 5001, Australia
Email: valeri.lenchine@epa.sa.gov.au

Abstract

Outdoor noise measurements can be highly affected by the wind-induced noise generated by turbulence structures present in the flow and wakes generated at the air and windshield interface. Various commercially available windshields were tested in a small anechoic wind tunnel in order to investigate the effects of turbulent flow properties on the wind-induced noise in shielded microphones. To distinguish the contribution of wind-induced noise from the acoustic signal an Incoherent Output Power analysis between two microphone signals has been used. The effects of mean flow velocity, turbulence intensity and average length scales on the wind-induced noise in shielded microphones were evaluated. An incremental trend with increasing airflow velocity has been found for the wind noise spectral amplitudes. The findings indicate a dependency between turbulent scales and the wind-induced noise levels at low frequencies. The overall wind-induced noise was found to be insensitive to the incoming flow turbulence intensity levels which may suggest that other parameters of the incoming flow turbulence, such as turbulence scale, are more important for the processes of wind-induced noise generation.

1. Introduction

The accuracy of noise measurements in outdoor environments in the presence of wind is reduced by wind-induced noise generation over the microphone due to turbulence structures present in the flow and microphone wake generated noise. Windshields are commonly utilised to reduce the unwanted effects of the wind-induced noise, however they have performance limitations over a broad range of flow conditions.

Wake generated noise due to laminar flow over the windshield is well understood, however there is relatively little research characterising the effects of different turbulent flow properties on the wind-induced noise generation in shielded microphones. This is of great importance due to the turbulent flow conditions frequently occurring in typical outdoor conditions.

This paper summarises the findings of a study attempting to characterise the effects of various flow conditions on the wind-induced noise generation in shielded microphones in a series of indoor tests in an anechoic wind tunnel.

2. Wind-induced noise

Wind-induced noise is caused by non-acoustic pressure fluctuations imposed on a microphone diaphragm and commonly known to comprise two major mechanisms: pressure fluctuations due to the interaction of a turbulence free flow over the microphone surface known in the literature as self-generated noise [1] or self-noise [2] or "pseudo-noise" [3]; and pressure disturbances due to existing eddy structures in the flow impinging on the microphone surface [1,4,5,6].

The contribution of these two mechanisms may vary based on the level of turbulence in the flow. For a turbulence-free flow, the dominant noise is due to the interaction of flow over the surface of the microphone [4,6]. However, in a highly turbulent flow the dominant pressure fluctuations on the microphone diaphragm may be mainly due to the eddy structures impinging on the windshield surface [4]. The interaction of turbulence structures impinging on the surface of the microphone has been noted as the dominant contributor to the wind-induced noise in shielded microphones in atmospheric conditions [4, 5].

A number of different studies were conducted in controlled environments with the aim of understanding the wind-induced noise generation processes and in particular self-generated noise. The dimensional analysis of Strasberg [1] summarises the effects of self-generated noise as a function of the windshield diameter, frequency and flow velocity based on measurements in laminar flow. The analysis shows a linear relationship between the logarithms of dimensionless one-third octave sound pressure level and Strouhal numbers below five. Here Strouhal number was defined as the product of frequency and windshield diameter divided by the flow velocity.

Leclercq, Cooper and Stead [2] have found from a series of anechoic wind tunnel measurements a 6^{th} power law dependence between self-noise and flow speed where an increase in flow speed will result in higher self-noise. Wang, Zander and Lenchine [7] estimated and characterised the wind-induced noise generation using Incoherent Output Power between two shielded microphones, one positioned inside the jet and another positioned outside the jet.

Various attempts have been made to characterise the wind-induced noise in shielded microphones in different atmospheric conditions. Morgan and Raspet [4] conducted an empirical study of wind noise in shielded microphones in outdoor environments indicating pressure disturbances in the incoming flow as the major contributor to wind noise in outdoor environments. They found that pressure fluctuations caused by incoming flow velocity variations are the dominant source in outdoor wind noise generation. However, they also indicate that in flow conditions where low levels of pressure fluctuations exist, this dominance shifts to the interaction of flow over the windshield surface and its associated wake generation (the mechanism which may contribute less in a highly turbulent flow).

Van den Berg [5] also studied wind-induced noise in shielded microphones in outdoor measurements and provided analytical expressions for wind noise corresponding to different atmospheric conditions. He concluded that outdoor wind noise in a shielded microphone is dependent not only on the average wind speed and windshield diameter, but also depends on atmospheric turbulence which is defined by thermal and frictional turbulence. Consequently, two other parameters associated with wind-induced noise were introduced by Van den Berg [5], which are defined by atmospheric conditions (i.e. atmospheric stability) and terrain properties (i.e. terrain roughness height).

Cooper, Leclercq and Stead [8] have undertaken atmospheric measurements of wind-generated microphone noise, and provided a relationship between wind speed and microphone-generated L_{Aeq} noise level for a range of wind shields. They suggest that the level of wind-induced noise under atmospheric turbulence is less than that measured using wind tunnel measurements. However, the study does not include any estimates of turbulent flow parameters.

The majority of the studies conducted to characterise wind-induced noise in shielded microphones appear to be mainly either conducted in low turbulence flow or have not addressed the turbulent flow parameters sufficiently. This paper aims to investigate the relationship between various turbulent flow properties and wind-induced noise generation in shielded microphones in a series of indoor tests in an anechoic wind tunnel.

3. Experimental arrangement

Different sized spherical windshields were tested in various flow conditions in a small anechoic wind tunnel in the School of Mechanical Engineering at the University of Adelaide. Wang, Zander and Lenchine [7] introduced the Incoherent Output Power analysis of two shielded microphones, one inside the flow and the other outside the flow to estimate the wind-induced noise in shielded microphones. This technique was further developed in a series of tests in an anechoic wind tunnel indicating the potential of this technique to estimate the wind-induced noise in different flow conditions [9].

The experimental arrangement consisted of a microphone equipped with a windshield located outside the flow in order to provide a reference signal and another microphone equipped with the same type of windshield mounted within the jet to capture the contribution of wind-induced noise. A loudspeaker was used to generate a white noise signal with overall sound pressure level (SPL) of approximately 106 dB in the audio frequency span for all acoustic measurements to generate coherent signals on both microphones with no flow and minimise the effect of background noise. Two B&K 4190 free field microphones equipped with windshields were utilised to perform the acoustic measurements. A multi-channel data acquisition system was used to record the microphone signals in different flow conditions and for each type of windshield. Results for different sized spherical windshields with diameter of 60 – 90 mm are examined in this paper.

The concept behind utilisation of IOP to estimate the wind-induced noise is that the loudspeaker signal can be thought of as the desired acoustic signal to be measured in outdoor conditions. The acoustic signal is contaminated by the wind-induced noise due to the unwanted pressure fluctuations caused by flow interaction over the windshield. IOP can then be utilised to extract the wind-induced noise from the total contaminated signal; i.e. the power of the response microphone that is incoherent with the reference microphone. Refer to Wang, Zander and Lenchine [7] and Alamshah, Zander and Lenchine [9] for further detail of the methodology and signal processing technique used.

Two different arrangements were utilised in this study to achieve higher turbulence intensity at various positions in the wind tunnel (Figure 1). The turbulence intensity was artificially increased by positioning different rectangular meshed grids upstream in the flow, and the streamwise position of the microphones was changed to downstream locations representing higher turbulence intensity.

The experimental arrangement incorporating meshed grids is shown in Figure 1. In this arrangement the leading edges of both reference and response microphone windshields were positioned at 200 mm from the jet exit plane.

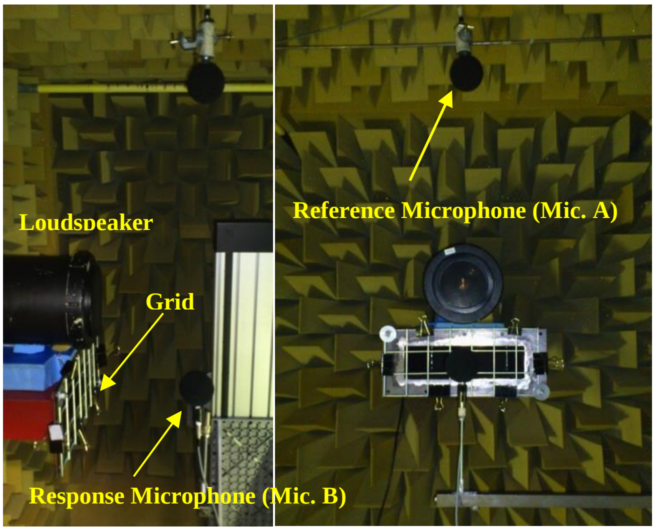

Figure 1. Experimental arrangement

Three different sized rectangular meshed grids with round wires were positioned at the contraction outlet. The geometry of the grids used in this experiment is shown in Figure 2. Further, the geometrical parameters for the grids are presented in Table 1.

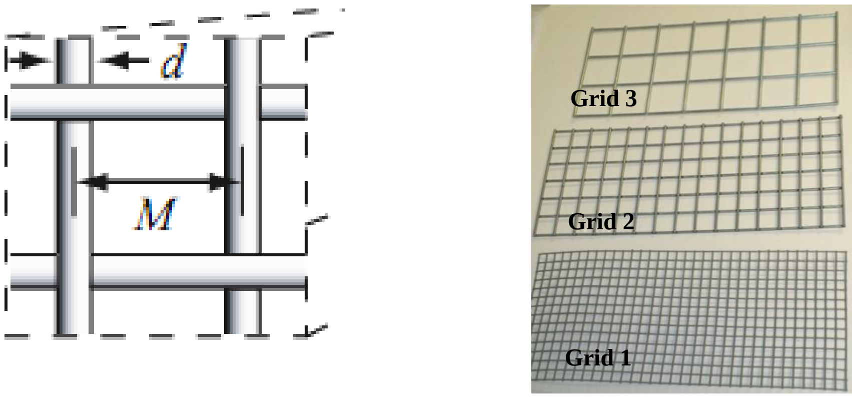

Figure 2. Turbulent generator grid geometry [10] and grids used in this study

Table 1. Grid geometry

Grid	*M* (mm)	*d* (mm)
1	11	1.5
2	25	3.2
3	50	3.9

Another way to control turbulence intensity at the position of the response microphone was to change the streamwise position of the response microphone in the free jet. Three streamwise positions of 200 mm, 400 mm and 600 mm downstream of the jet exit plane were chosen to investigate the effect of higher turbulence levels without any grids present.

Hotwire anemometry was conducted to characterise the flow properties of the wind tunnel jet. Instantaneous velocity values were obtained at various locations using the hotwire survey and were processed to obtain the mean flow velocity, turbulence intensity and the integral length scale. Turbulence intensity in the mean flow direction is defined as [11]

$$Tu = \frac{u_{rms}}{\overline{U}} \tag{1}$$

where u_{rms} is the root mean square of the mean flow velocity fluctuation and is equal to the standard deviation of the instantaneous velocity samples. Integral length scales were estimated using a frozen turbulence approximation [12] where spatial correlations are estimated from the temporal correlations. The longitudinal integral length scale, which is a measure of longest connection or correlation distance between the velocities at two points in the flow is defined as [13,14]

$$L_u(x,t) = \frac{1}{R_{uu}(0,x,t)} \int_0^\infty R_{uu}(e_u r, x, t) dr \tag{2}$$

where

$$R_{uu}(r,x,t) \equiv \langle u(x,t) u(x+r,t) \rangle \tag{3}$$

is the spatial correlation function of the longitudinal velocity component, u, between two points with distance r, and e_u is the unit vector in the mean flow direction. Based on the frozen turbulence approximation, the integral length scale can be approximated as

$$L_u(x,t) = \frac{\bar{U}}{R_{uu}(x,0)} \int_0^{\infty} R_{uu}(x,\tau)d\tau \tag{4}$$

where

$$R_{uu}(x,\tau) \equiv \langle u(x,t)u(x,t+\tau)\rangle \tag{5}$$

is the temporal autocorrelation function of the longitudinal velocity component, u, at a given location, x, and $\bar{U}$ is the mean flow velocity in the mean flow direction. Equation 4 requires integration of the autocorrelation function over an infinite domain. In practice this is not possible. The integration domain used here is from zero to the first zero crossing of the autocorrelation function [15]. Note that the normalised temporal autocorrelation function of the fluctuating velocity component, u, represents the integral time scale in the mean flow direction.

A traverse allowed continuous movement of the hotwire anemometry in different directions. Figure 3 shows the mean velocity and turbulence intensity along the centreline of the jet at different free stream velocities indicating approximately constant velocity up to the 350 mm downstream of the exit plane and incremental turbulence intensity as a function of streamwise distance increasing to values as high as 16 to 18 % at 600 mm from the jet exit plane.

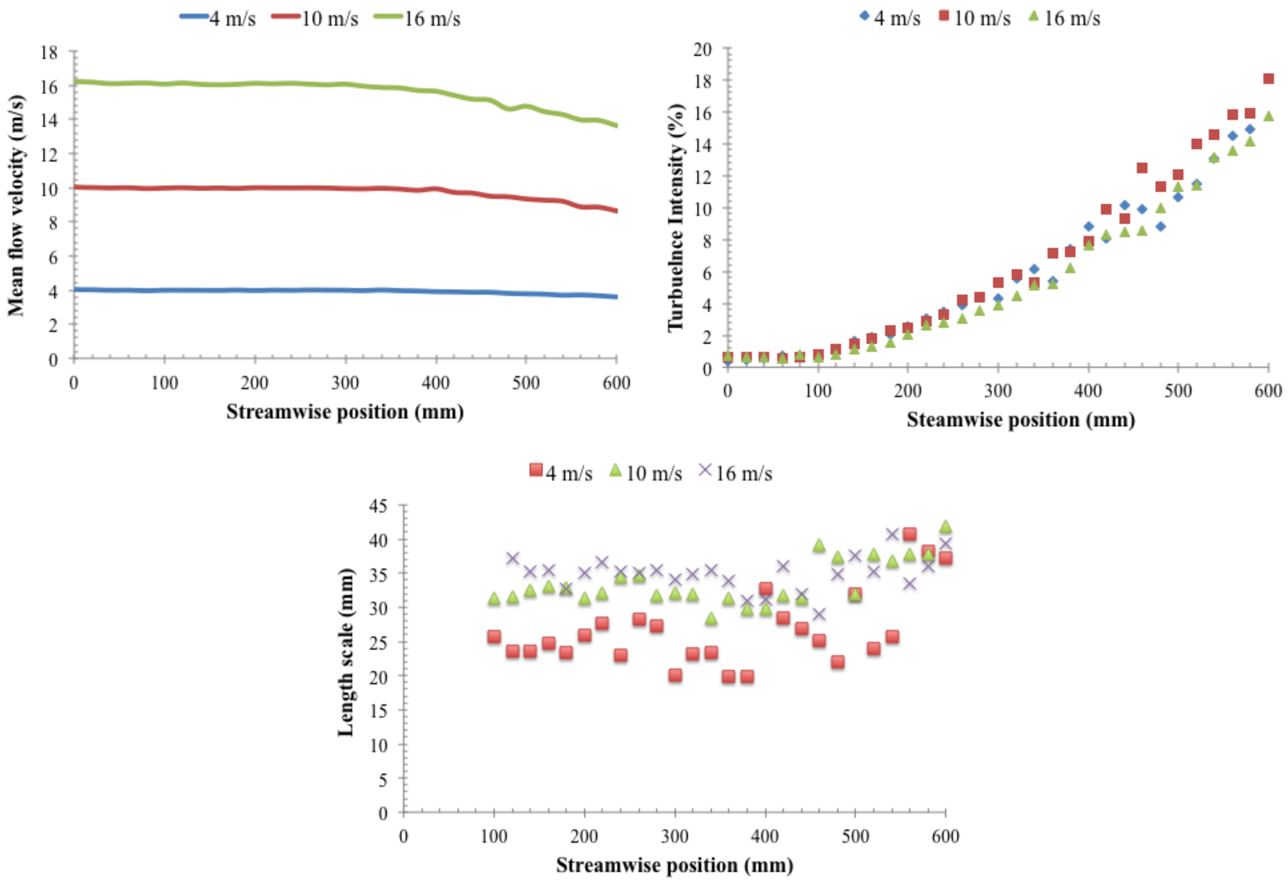

Figure 3. Free jet mean flow velocity (top left), turbulence intensity (top right) and length scale (bottom) as a function of distance from the jet exit plane at different free stream velocities

Different flow property profiles at 200 mm from the jet exit plane are shown in Figure 4 for various free stream velocities. The mean velocity shows an approximately uniform velocity profile within 20 mm of the centreline of the jet. The turbulence intensity increases in the direction normal to the mean flow ranging from 2 % to values as high as 50 %. The length scale appears to decrease from the centre line in the direction normal to the flow to about 40 – 50 mm from the centre line and increases again above that point. Figure 5 presents different flow properties measured at the centreline of the jet and averaged over the projected area of the 90 mm windshield for different turbulence generating grids indicating, an increase in the average turbulence intensity and higher estimated length scales for the free jet compared to the various grids over the area of the windshield with different grids used. Similar trends were found with windshields of other diameters.

It is noted that smaller or similar average length scales are measured for coarser grids (i.e. Grids 2 and 3) compared to finer grid used (i.e. Grid 1). For a homogeneous isotropic turbulence, a larger length scale is expected for coarser mesh wire spacing (i.e. larger *M*) [10]. The measured smaller length scales for Grid 2 and 3 compared to Grid 1 may have been due to uneven distribution of mesh grids over the area of the wind tunnel contraction outlet for coarser grids compared to finer grid resulting in variation in mesh wire spacing due to installation limitations imposed by the wind tunnel contraction.

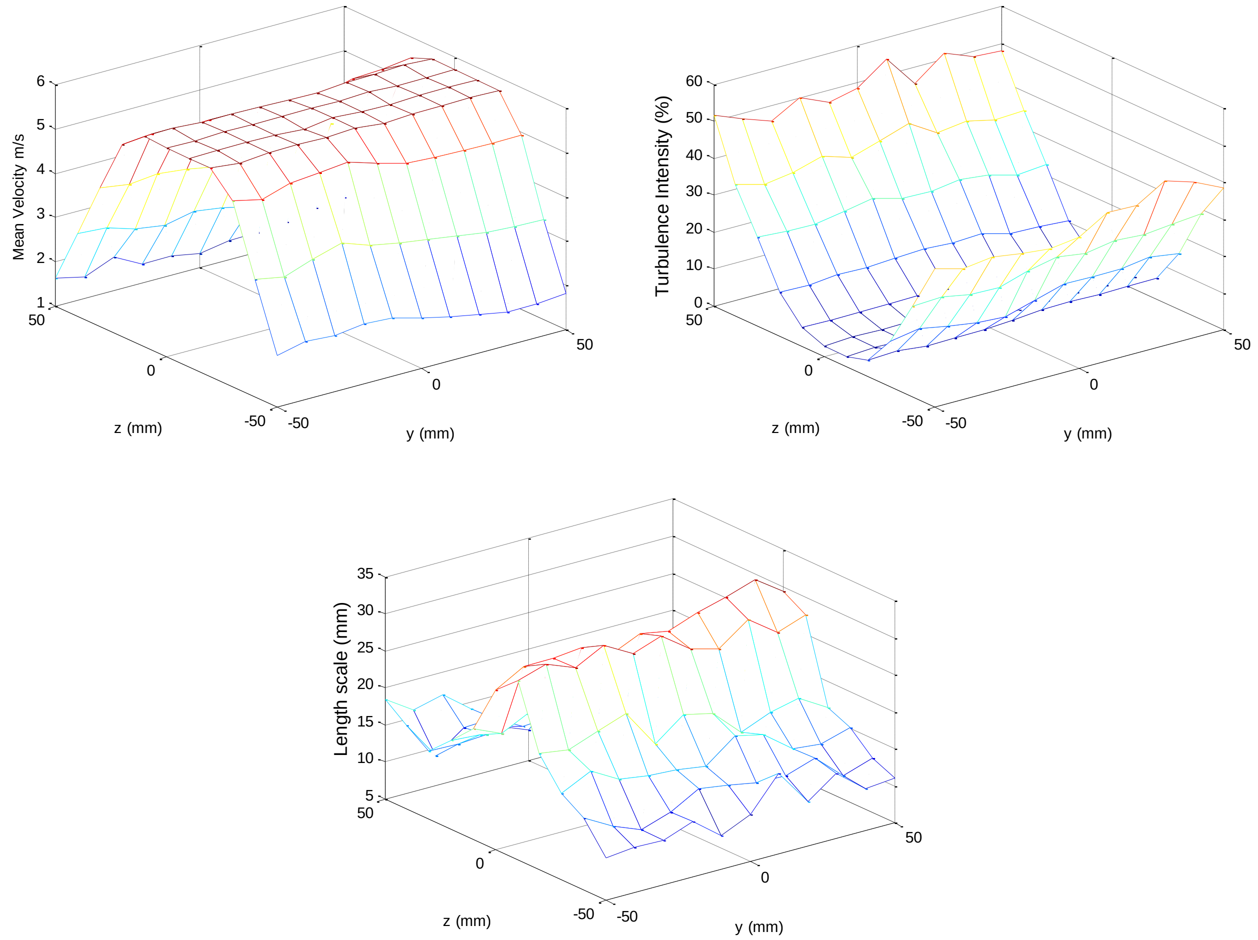

Figure 4. Free jet mean airflow velocity (top left), turbulence intensity (top right) and length scale (bottom) profiles at 200 mm from the jet exit plane at a free stream velocity of 6 m/s. Graph origin is the jet centreline

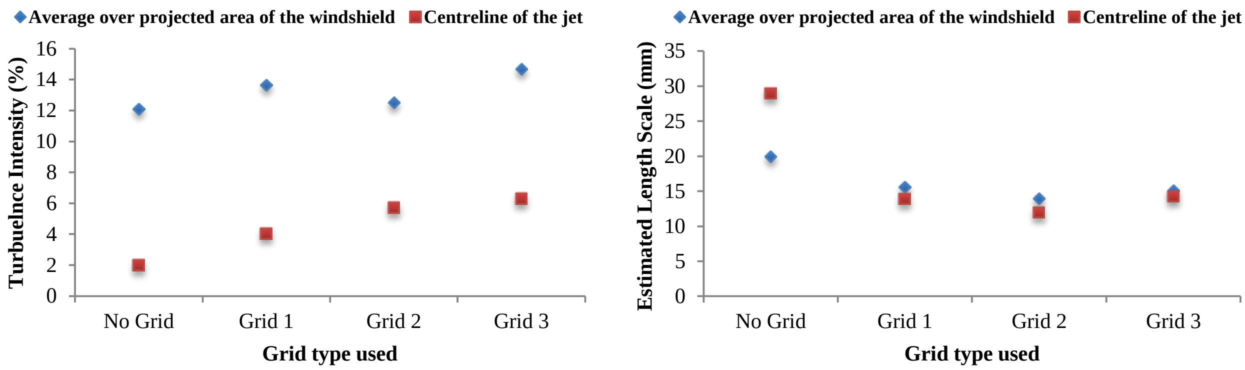

Figure 5. Free jet turbulence intensity (left) and estimated length scale (right) measured at 200 mm from the exit plane for 90 mm windshield at a free stream velocity of 6 m/s

4. Results

4.1 Wind-induced noise and airflow velocity

Figure 6 shows the effect of various airflow velocities on the Incoherent Output Power representing the wind-induced noise for selected windshields of 60 mm and 90 mm diameter tested in the free jet. For these measurements the leading edges of the windshields were positioned at 200 mm from the jet exit plane where the average turbulence intensity of about 2 % was measured at the centreline of the jet (see Figure 4). The wind-induced noise demonstrates a similar pattern among different windshield types at different velocities. Generally wind noise increases with the mean airflow velocity where the rate of the level change decreases as velocity increases. This is evident from the spacing of different velocity lines which are closer to each other in the 12 to 30 m/s velocity range. Increase in wind-induced noise with increase in the airflow velocity is well explored [1,2,4,5,7,8,10]. The overall wind-induced noise level for a specific windshield diameter appears to be proportional to the logarithm of airflow velocity which is in agreement with the literature [1,2,5,8].

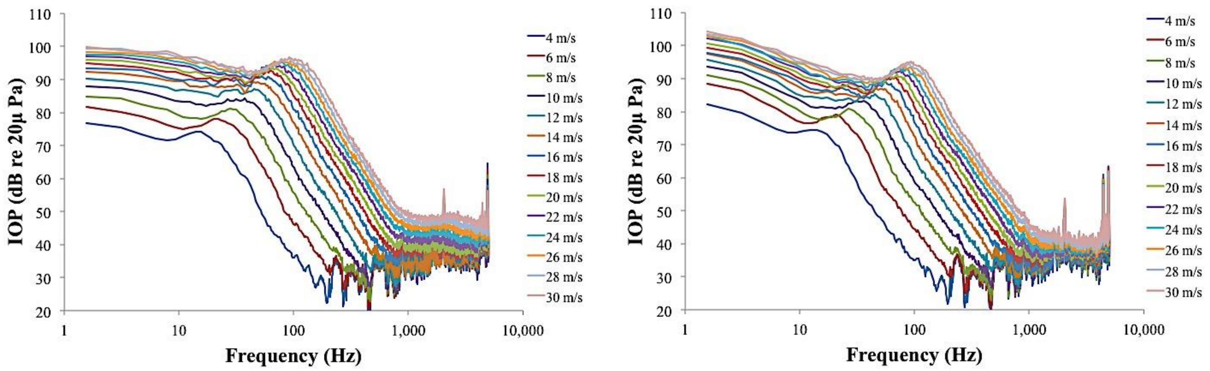

Figure 6: Wind-induced noise for 60 mm (left) and 90 mm (right) diameter windshields at different velocities

It can be seen from Figure 6 that the frequency span of the wind-induced noise at different airflow velocities can be separated into three regions: one being a low frequency region (typically less than 40 Hz for velocities less than 30 m/s) where the wind-induced noise does not appear to change significantly with respect to frequency. This is consistent with previous studies indicating a low frequency region of wind-induced noise spectra being independent of frequency [5]. The other region appears to be a local maximum in the low to mid frequency range where the trend changes, and the third region of wind-induced spectra which is characterised by an almost linear decrease of the levels proportional to the logarithm of the frequency which is consistent with the findings of other studies [2,5,7]. The wind induced noise at higher frequencies outside of these three regions is sufficiently low that the levels are most likely affected by instrument noise.

It appears from Figure 6 that the wind-induced noise generated in 90 mm windshield, in particular in low frequencies, is higher than the 60 mm windshields at the same airflow velocity. This may be due to the fact that larger windshield is exposed to regions of higher turbulence intensity at the edge of the windshield.

4.1 Artificially generated turbulence

Figure 7 shows the measured IOP representing the wind-induced noise for a 90 mm diameter windshield at two different velocities and a variety of girds positioned upstream of the flow with the intention of controlling the turbulence properties of the flow. It can be seen that at low and mid frequencies the wind-induced noise for the free jet (i.e. “No grid”) is typically higher than other cases where the grids were used to increase the turbulence intensity. Both the average turbulence intensity over the projected surface of the corresponding windshield (see Figure 5) and the turbulence intensity measured at the centre of the jet (see Figure 5) for the free jet stream show lower values than for the case where the grids are mounted at the nozzle outlet. However, the integral length scales for the free jet stream (both averaged over the projected surface and measured at the centre of the jet at x = 200 mm) show relatively higher values compared to the case where grids are inserted in the flow.

It is noteworthy to mention that generally the free jet mean flow profiles were more uniform compared to the flow profiles of those with the grids installed upstream. This may indicate that the averaging mechanism which enhances the cancellation of the pressure fluctuations at the interior of the windshield, is less effective as there is less chance of pressure cancelation due to flow uniformity. The results may also suggest that the higher wind induced noise for the free jet (i.e. “No grid”) may be associated with the larger eddy scales impinging on the surface of the windshield. This might explain the higher values of wind-induced noise for the windshields positioned in the free jet compared to those with grids installed upstream. Similar wind noise spectra trends were found for the other diameter windshields used.

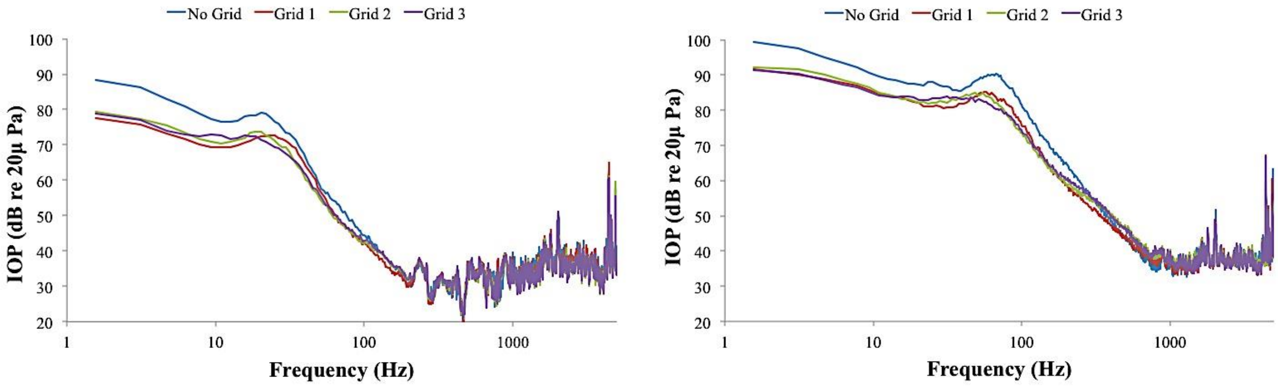

Figure 7: Wind noise for 90 mm diameter windshield at airflow velocities of 6 m/s (left) and 18 m/s (right) with different grids positioned upstream

The wind noise spectra shown in Figure 7 illustrate similar levels for different grids positioned upstream from the windshields. Although the turbulence intensity for grids 1 to 3 increases slightly and the integral length scale stays within a narrow range, the wind-induced noise spectra are approximately the same within 1 – 2 dB error. It seems that the wind induced noise is not sensitive to the turbulence intensity variations within the range of the magnitude explored in this study. Similar spectral shape with local maximum for the wind induced noise can be observed for no grid and grids 1 to 3 experimental arrangements. The local maximum frequency does seem to slightly shift to lower frequencies as the turbulence intensity and the integral length scales increase. It should be noted that the turbulent flow characterisation of incoming flow over the windshield surface is done without the presence of the windshields in the flow, which indeed significantly affects the near flow field characteristics.

4.2 Free jet increased turbulence

The position of microphones equipped with different windshields were changed within the free jet stream to achieve higher turbulence intensity levels over the surface of the windshields. The leading edges of the windshields were positioned at 200 mm, 400 mm and 600 mm from the jet exit plane in the streamwise direction.

The wind-induced noise spectra for different streamwise positions and airflow velocities for a 90 mm diameter windshield are shown in Figure 8. The flow characterisation shown in Figure 3 shows that the turbulence intensity measured at the centreline of the jet has significantly increased from a value of about 2 % at 200 mm from the jet exit plane up to values of about 15 – 18 % at 600 mm from the jet exit plane for various airflow velocities. The integral length scale measured at the centreline of the jet also increased by about 5 mm to 10 mm as the position of the microphone is shifted from 200 mm to 600 mm from the jet exit plane (see Figure 3). The increase in the turbulence intensity and the integral length scale seem to have resulted in increase in the level of the local maximum (or trend change point) in the wind noise spectrum. Further the local maximum frequency has also shifted to lower frequencies as the turbulence intensity and scales were increased for a specific windshield type and airflow velocity. This was also observed for turbulence generated with grids to a lesser degree. This shift in local maximum frequency tends to higher frequencies as the mean airflow velocity increases. The wind noise spectra for other tested windshields also illustrates similar behaviour in response to the increased turbulence intensity and scales in the flow.

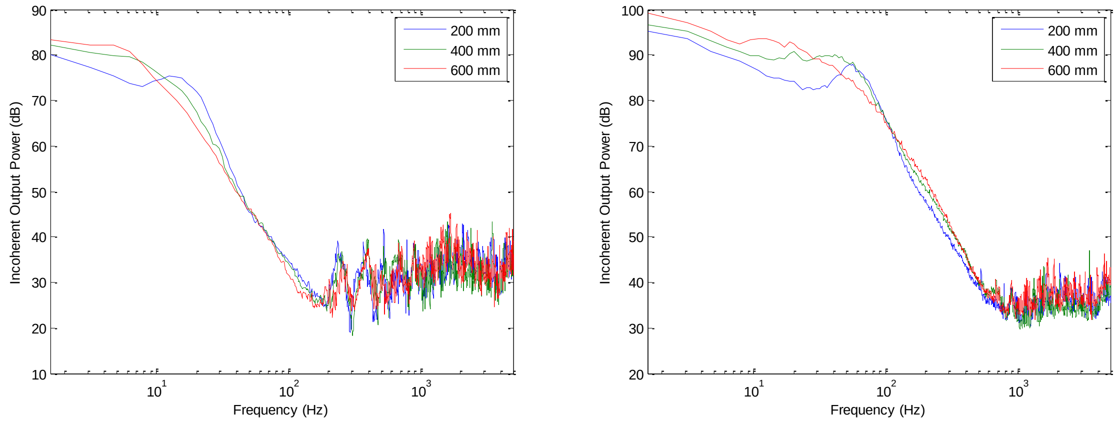

Figure 8: Wind-induced noise for 90 mm windshield at different positions streamwise of the jet for airflow velocity of 4 m/s (left) and 16 m/s (right)

The wind noise spectra corresponding to the rapid decay region of the wind noise (i.e. frequencies above the local maximum) are similar within 3 dB at different streamwise positions of the microphones. This suggests that the increase in the turbulence intensity and the integral length scale within the range observed during the experiments may not considerably affect the higher frequency noise generation. Increased turbulence intensity and length scale appears to increase the low frequency component of the wind-induced noise as well as shifting the frequency of the local maximum to lower values. This is particularly important in infrasonic or low frequency noise measurements outdoors where the smallest turbulent structures in the flow could potentially contaminate the frequencies of interest.

Despite the significant increase in the measured turbulence intensity and increase in the integral length scale, the overall wind noise does not increase significantly (an increase of about 3 dB was observed at the highest turbulence conditions). This indicates that increase in the incoming flow turbulence parameters within the explored range does not significantly affect the wind noise for a specific windshield type and diameter. This may suggest that the incoming flow turbulence may not be the major contributor to the wind-induced noise generation in shielded microphones, as the increase in incoming flow turbulence intensity or scale does not noticeably increase the wind induced noise. This is not in good agreement with the findings of the literature, which indicate the incoming flow turbulence as the major contributor to the wind noise in highly turbulent flows occurring in outdoor conditions [4,5].

It should be noted that the findings of the literature indicating the domination of incoming flow turbulence as the contributor to the wind-induced noise compared to the self-generated noise (due to interaction of predominantly laminar flow with the wind shield) are mainly based on outdoor noise measurements [4,5]. While the findings of the current study are based on a series of indoor experiments conducted in a controlled environment.

Further it is acknowledged that the behaviour of a turbulent free jet or artificially generated turbulent flow using grids is considerably different from the atmospheric boundary layer where outdoor measurements are conducted. However, the findings of this study might be to some extent comparable with the turbulent flow characteristics of the atmospheric surface layer where the mechanical turbulence (i.e. frictional turbulence) dominates over the convective turbulence [16].

Another noticeable difference between the atmospheric turbulent flow and the free turbulent jet is that the length scales produced in this study by the free jet were much smaller than that of a turbulent flow in the atmospheric surface layer. The flow characterisation of the free jet stream has shown that the average length scales estimated using the integral length scales are typically smaller than the diameters of the windshields tested in this study. This is less likely to be the case in outdoor noise measurements.

It is noted that the mechanism and behaviour of the wind-induced noise generation due to the interaction of turbulent structures generated artificially by positioning the grids upstream of the windshields does in fact seem to be different from that of turbulent structures within a free jet. Admittedly, this was expected as the flow behaviour of a free jet stream is different from that of artificially generated turbulence using meshed grids.

Another interesting similarity between the two cases is that the local maximum frequency shifted to lower frequencies for both artificially increased turbulence as well as for the free jet conditions with increased turbulence intensity. This might indicate that the shift in the local maximum frequency is associated with the increase in turbulence intensity which seems to be the common flow trend among the two cases (i.e. average length scales for artificially increased turbulence were roughly the same for a specific case).

6. Conclusions

The effects of increased mean flow velocity, turbulence intensity and average length scales on the wind-induced noise generation in shielded microphones were evaluated. An incremental trend with increasing airflow velocity was found for the wind noise spectral magnitudes. The effect of increased flow turbulence levels using artificially increased turbulence as well as various positioning of the microphones in a free jet were investigated. For both cases the wind-induced noise at very low frequencies appears to increase with increasing average length scales within the flow. Increase in turbulence intensity did not seem to have a considerable effect on the wind-induced noise levels.

In summary, the results of increased turbulence levels indicate a dependency between turbulent scales and increase in the wind-induced noise levels at low frequencies. In addition, the overall wind-induced noise was found to be less sensitive to change in the incoming flow turbulence intensity. This may be connected to the limited range of turbulence intensities and scales reproduced during the experiments. The integral turbulence scale was significantly less than the characteristic dimensions of the wind shields. Nevertheless, a definitive conclusion cannot be drawn and further study is deemed necessary to account for the complex nature of turbulent structures impinging on the surface of the windshield.

Acknowledgements

The authors thank the SA Environment Protection Authority for their support of this work. Thanks also to Professor Graham Nathan, Dr Danielle Moreau and Jonathan Cooper for their guidance and valuable feedback during this work.

References

[1] Strasberg, M. "Dimensional analysis of windscreen noise", *Journal of the Acoustical Society of America*, **83**, 544-548, (1988).

[2] Leclercq, D, Cooper, J and Stead, M. "The use of microphone windshields for outdoor noise measurements", *Proceedings of Acoustics 2008*, Geelong, Victoria, Australia, 24-26 November 2008.

[3] Pearse, JR and Kingan, MJ. "Measurement of Sound in Airflow", *Proceedings of the 13th International Congress on Sound and Vibration* (ICSV13), Vienna, Austria, 2-6 July 2006.

[4] Morgan, S and Raspet, R. "Investigation of the mechanisms of low-frequency wind noise generation outdoors", *Journal of the Acoustical Society of America*, **92,** 1180-1183, (1992).

[5] Van den Berg, G. "Wind-induced noise in a screened microphone", *Journal of the Acoustical Society of America*, **119**, 824-833, (2006)

[6] Zheng, ZC and Tan, BK. "Reynolds number effects on flow/acoustic mechanisms in spherical windscreens", *Journal of the Acoustical Society of America*, **113**, 161-166, (2003).

[7] Wang, L, Zander, AC and Lenchine, VV. "Measurement of the Self-Noise of Microphone Wind Shields", *Proceedings of 18th Australasian Fluid Mechanics Conference*, Launceston, Tasmania, Australia, 3-7 December 2012.

[8] Cooper, J, Leclercq, D and Stead, M. "Wind induced aerodynamic noise on microphones from atmospheric measurements", *Proceedings of the 20th International Congress on Acoustics* (ICA2010), Sydney, Australia, 23-27 August 2010.

[9] Alamshah, SV, Zander, AC and Lenchine VV. "Development of a technique to minimise the wind-induced noise in shielded microphones", *Proceedings of Acoustics 2013*, Victor Harbor, South Australia, Australia, 17-20 November 2013.

[10] Kurian, T and Fransson JHM. "Grid-generated turbulence revisited", *Fluid dynamics research*, **41**, 021403, (2009).

[11] Bruun, HH. *Hotwire anemometry: principles and signal analysis*, Oxford University Press, New York, USA, 1995.

[12] Taylor, GI, "The spectrum of turbulence", *Proceedings of the Royal Society of London, Series A-Mathematical and Physical Sciences*, **164**, 476 – 490, (1938).

[13] Hinze, JO, *Turbulence: An introduction to its mechanism and theory*, McGraw-Hill, New York, USA, 1975.

[14] Pope, SB, *Turbulent Flows*, Cambridge University Press, Cambridge, United Kingdom, 2000.

[15] O'Neill, P, Nicolaides, D, Honnery, D and Soria, J "Autocorrelation functions and the determination of integral length with reference to experimental and numerical data", *Proceedings of the 15th Australasian Fluid Mechanics Conference*, Sydney, Australia, 13-17 December 2004.

[16] Panosfsky, HA and Dutton, JA, *Atmospheric turbulence: models and methods for engineering applications*, John Willey & Sons, USA, 1984.